Direct Torque Control of Dual Stator Winding Induction Machine based on PI-Sliding Mode Control

Mojtaba Ayaz
PhD Candidate
Electrical engineering department
Ferdowsi university of Mashhad
Mashhad, Iran
mojtaba.ayaz@mail.um.ac.ir

Hossein Abootorabi
Assistant professor
Electrical engineering department
Ferdowsi university of Mashhad
Mashhad, Iran
Abootorabi@um.ac.ir

Abstract— **This paper presents a Direct Torque and flux Control (DTC) system for a Dual Stator Winding Induction Machine (DSWIM). The proposed DTC is based on PI-sliding mode control (PI-SMC) and benefits both linear and variable structure controllers to have an appropriate operation both in steady state and transient operation conditions. The reference values of fluxes are selected to satisfy maximum torque per Ampere (MTPA) strategy and the torque reference values are determined by an innovative torque sharing algorithm. This algorithm ensures wide speed range operation, including zero speed. The proposed control system is validated using MATLAB/SIMULINK. The simulation results confirm that the proposed control system has an admirable performance from rated positive to rated negative speed range.**

Keywords-component; Dual Stator Winding Induction Machine (DSWIM), Direct Torque Control, PI-Sliding Mode Control, MTPA, Wide speed range control.

I. INTRODUCTION

Squirrel cage three phase induction machines are broadly utilized in various industrial applications. Since they have robust and simple structure and they are able to operate in different environmental conditions, including polluted and explosive environments. In addition, unlike synchronous machines, they have self-starting torque and no starting method is required. Moreover, they are relatively low-cost electrical machines and involve low maintenance operation. Despite the valuable above mentioned advantages, three phase induction machines show inconvenient operation in low speed ranges, especially when they are derived by sensorless controllers.

To overcome this limitation, Lipo et al added a secondary three phase winding to the stator of a squirrel cage three phase induction machine and introduced the Dual Stator Induction Machine (DSWIM) [1]. In fact, a DSWIM has two sets of three phase windings with dissimilar pole numbers in its stator and its rotor is a standard squirrel cage one. If two winding sets are fed by voltage sources having the frequency ratio equal to the pole number ratio and localized saturation is avoided, the operation of two winding sets is independent [2]. This machine involves low-cost and simple construction in comparison to other kinds of dual winding induction machines, as BDFIM [3]. Moreover, it has high reliability and robustness in comparison with single winding three phase induction machines. In addition, its operation is highly controllable in a wide speed range, including zero speed.

The DSWIM has found applications in various motoring and generating applications. In [4] a DSWIM is utilized for DC generation system. In this application the power produced by each winding set is rectified through separate PWM rectifiers and a vector control system is proposed to have minimum copper loss in the generation system. In [5] a vector control system based on IOFL strategy is proposed for the same application. The proposed strategy is validated for both series and parallel connections of the DC power produced by each winding sets.

In [1] a DSWIM with 1:3 pole ratio is introduced for motoring application and scalar and direct vector control systems are proposed for controlling the rotor speed in a wide speed range including zero speed. In this paper two operating modes are introduced: synchronous operation and asynchronous operation. In the synchronous operation the supply frequencies to winding sets has a ratio equal to the pole numbers ratio and this operation mode is utilized for high rotor speed ranges. In asynchronous operation mode which is utilized in low speeds, the supply frequency of one of the winding sets is kept at a low value (2.5 Hz). However, utilizing this control strategy results in localized saturation and additional core losses in low speed ranges. In [6] an indirect vector control system is proposed for DSWIM in motoring operation. In the proposed control system, the supply frequency of one of the winding sets is also kept constant and the supply frequency of the other winding is controlled such that the required torque for the output load is provided. In [7] an indirect vector control system is proposed too. In addition, an MRAS speed estimation and flux observer is proposed to ensure system stability in various load conditions.

As mentioned before, in order to have independent control systems in each winding sets of a DSWIM, the localized saturation must be shunned. References [8-11] propose strategies for flux level selection in a DSWIM in order to avoid saturation and optimize machine operation. In [8] the flux level selection of each winding set is selected such that MTPA condition is obtained. In the proposed control system, which is an indirect vector control system, torque sharing between winding sets is done such that the relative position of fluxes produced by winding sets is kept optimal. The operation of the

978-1-5386-4916-9/18/$31.00 ©2018 IEEE

proposed control system is limited to high positive or negative speed ranges. Moreover, this control strategy is highly parameter dependent and requires precious positioning of individual fluxes produced by each winding set.

In this paper a direct torque controller is proposed for DSWIM. The proposed control scheme is based on PI-Sliding mode control to satisfy appropriate dynamic and steady state responses. In the proposed control system the reference values of fluxes for winding sets are selected to avoid saturation and execute MTPA strategy. Furthermore, the torque reference values are determined such that wide speed range operation is achieved.

The rest of this paper is organized as follows: the DSWIM modeling is presented in section II. The proposed control system is described in section III. Section IV is assigned to reference flux and torque selection. Section V presents the simulation results and section VI concludes the paper.

II. DSWIM Modeling

Dual Stator Winding Induction Machine (DSWIM) has two sets of three phase windings with dissimilar pole numbers in its stator and its rotor is a standard squirrel cage one. If the stator winding sets are supplied by voltage sources which have frequencies with the same ratio as the number of poles ratio, there is no coupling between two winding sets. Consequently, the DSWIM can be considered as two independent three phase induction machine, coupled by a common rotor.

Actually, any combination of dissimilar pole numbers can be chosen, but in order to have a high efficient DSWIM and avoid saturation it is suggested to choose 1:3 as the pole number ratio [1]. Therefore, the model of a DSWIM with two pole and six pole winding sets is used in this paper, the model of which in the synchronous reference frame is given as follows:

$$V_{S_i} = R_{S_i} I_{S_i} + \frac{d\lambda_{S_i}}{dt} + j\omega_{S_i}\lambda_{S_i} \tag{1}$$

$$V_{R_i} = R_{r_i} I_{r_i} + \frac{d\lambda_{r_i}}{dt} + j\left(\omega_{S_i} - \omega_r\right)\lambda_{r_i} = 0 \tag{2}$$

$$\lambda_{S_i} = L_{S_i} I_{S_i} + L_{m_i} I_{r_i} \tag{3}$$

$$\lambda_{r_i} = L_{m_i} I_{S_i} + L_{r_i} I_{r_i} \tag{4}$$

For i=1 and 2.

Where i=1 and i=2 stand for two pole and six pole winding sets, respectively. V_{S_i} and V_{R_i} are the vectors of stator and rotor voltages in the ith winding sets, respectively. R_{S_i}, L_{S_i} and L_{m_i} represent the resistance, the self and mutual inductances of the ith winding set, respectively. R_{r_i} and L_{r_i} are the rotor resistance and inductance referenced at the ith winding. λ_{S_i} and λ_{r_i} are the vectors of stator and rotor fluxes in the ith winding sets respectively. ω_{S_i} and ω_r stand for synchronous speed of the ith winding and rotor speed, respectively.

The dq voltage and flux equations are as follows:

$$V_{S_i d} = R_{S_i} I_{S_i d} + \frac{d\lambda_{S_i d}}{dt} - \omega_{S_i}\lambda_{S_i q} \tag{5}$$

$$V_{S_i q} = R_{S_i} I_{S_i q} + \frac{d\lambda_{S_i q}}{dt} + \omega_{S_i}\lambda_{S_i d} \tag{6}$$

$$V_{r_i d} = R_{r_i} I_{r_i d} + \frac{d\lambda_{r_i d}}{dt} - (\omega_{S_i} - \omega_r)\lambda_{r_i q} = 0 \tag{7}$$

$$V_{r_i q} = R_{r_i} I_{r_i q} + \frac{d\lambda_{r_i q}}{dt} + (\omega_{S_i} - \omega_r)\lambda_{r_i d} = 0 \tag{8}$$

$$\lambda_{S_i d} = L_{S_i} I_{S_i d} + L_{m_i} I_{r_i d} \tag{9}$$

$$\lambda_{S_i q} = L_{S_i} I_{S_i q} + L_{m_i} I_{r_i q} \tag{10}$$

$$\lambda_{r_i d} = L_{m_i} I_{S_i d} + L_{r_i} I_{r_i d} \tag{11}$$

$$\lambda_{r_i q} = L_{m_i} I_{S_i q} + L_{r_i} I_{r_i q} \tag{12}$$

Considering $\lambda_{S_i} = \lambda_{S_i d}$ and $\lambda_{S_i q} = 0$, the electromagnetic torque produced by each winding is:

$$T_{e_i} = \frac{3}{2} P_i I_{S_i q} \lambda_{S_i} \tag{13}$$

Where P_i is the pole number of the ith winding. The total electromagnetic torque produced by the DSWIM is:

$$T_e = T_{e_1} + T_{e_2} \tag{14}$$

III. DTC Control of DSWIM

Generally speaking, DTC control refers to any control method that controls the torque and the stator flux independently, simultaneously and without using any decoupling medium. The general scheme of a DTC controller of an induction machine is illustrated in Fig.1. In this controller the torque and stator flux (or their estimated values) are compared with their reference values (referred by T_e^* and λ_s^*) and the resultant errors are passed through torque and flux controllers and produce the reference values of the direct and quadrature voltages (V_{sd}^* and V_{sq}^*) for the Voltage Source Inverter (VSI). Accordingly, VSI applies a set of three phase voltages to the stator winding such that the errors of the torque and the stator flux cancels.

The first generation of torque and flux controllers in a DTC controller were hysteresis ones [12]. These types of controllers have quick and robust response and they could be easily implemented by digital processors. However, the torque and flux

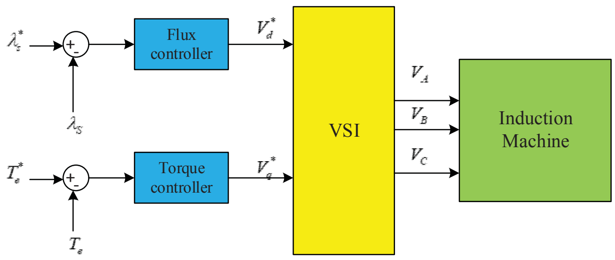

Figure 1. the general scheme of a DTC controller

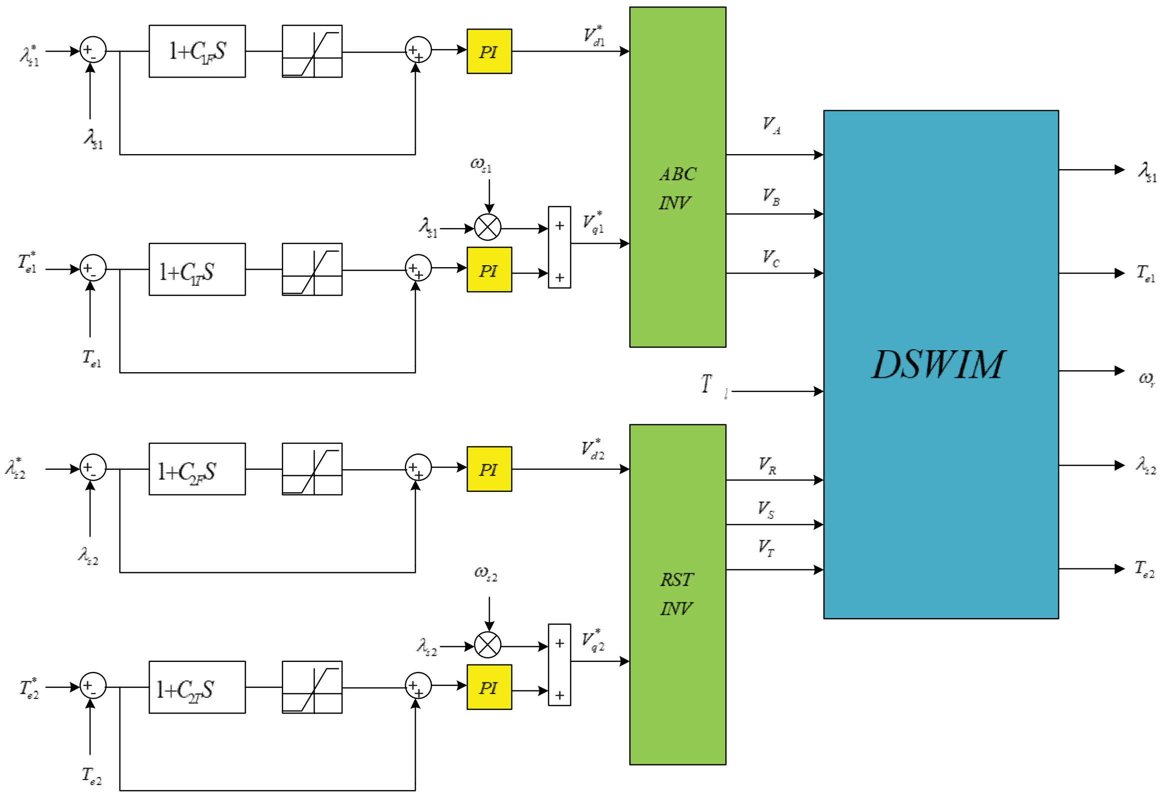

Figure 2. the proposed PI-SMC for DSWIM

ripples are relatively high. Moreover, their performance in in low speeds is undesirable. To surmount these disadvantages, linear torque and flux controllers are suggested [13]. Linear controllers show ripple free operation and they have very good dynamic response. Nevertheless, they cannot guarantee robustness. On the contrary, other types of torque and flux controllers which utilize Variable Structure Control (VSC), guarantee control robustness, but they result in large torque ripples [15]. To benefit the advantages of both linear and VSC type controllers a ((linear and variable structure control)) is proposed in [14]. This controller is a PI- Sliding Mode Controller (SMC), in which the PI controller is responsible for the transient operation and the SMC is dominant in the steady state operation.

In this paper this type of DTC controller is developed for a DSWIM. Figure 2 represents the proposed control scheme.

In equation (5) if $\lambda_{s_i} = \lambda_{s_i d}$ and $\lambda_{s_i q} = 0$, the variation of λ_{s_i} equals:

$$\frac{d\lambda_{s_i}}{dt} = V_{s_i d} - R_{s_i} I_{s_i d} \tag{15}$$

Therefore, the variation of λ_{s_i} is determined by $V_{s_i d}$. The stator quadrature axis current is:

$$I_{s_i q} = \frac{1}{R_{s_i}}\left(V_{s_i q} - \omega_{s_i}\lambda_{s_i}\right) \tag{16}$$

From (16) the electromagnetic torque equation can be rewritten as:

$$T_{e_i} = \frac{3}{2} P_i \frac{1}{R_{s_i}}\left(V_{s_i q} - \omega_{s_i}\lambda_{s_i}\right)\lambda_{s_i} \tag{17}$$

From (17) the electromagnetic torque produced by the ith winding set can be controlled by its quadrature axis voltage. However, there is a coupling between the torque and stator flux, which is $-\omega_{s_i}\lambda_{s_i}$. Consequently, as shown in figure 2 the quadrature axis voltage adds up with a decoupling term $(\omega_{s_i}\lambda_{s_i})$ to cancel this disturbance.

As discussed in section II, if the supply voltages of the two winding sets have the frequency ratio equal to the pole number ratio, there is no coupling between two winding sets. Accordingly, the proposed controller (shown in figure 2) has two distinct parts. Each part is responsible for controlling the torque and flux of one of the winding sets. Each controller is comprised of a switching controller, which is a SMC and a PI controller.

A. *The proposed SMC*

In the SMC the sliding surfaces is defined as:

$$S_i = S_{\lambda_{s_i}} + jS_{T_i} \tag{18}$$

In (18) $S_{\lambda_{si}}$ and S_{T_i} are defined as:

$$S_{\lambda_{S_i}} = e_{\lambda_{S_i}} + k_{\lambda_{S_i}} \frac{de_{\lambda_{S_i}}}{dt} \quad (19)$$

$$S_{T_i} = e_{T_i} + k_{T_i} \frac{de_{T_i}}{dt} \quad (20)$$

Where $e_{\lambda_{si}}$ and e_{T_i} represent the deviation from reference flux and torque, respectively.

$$e_{\lambda_{S_i}} = \lambda_{S_i}{}^* - \lambda_{S_i} \quad (21)$$

$$e_{T_i} = T_{e_i}^* - T_{e_i} \quad (22)$$

$k_{\lambda_{si}}$ and k_{T_i} are the SMC control parameters and they are selected such that the desired dynamics are obtained in SMC.

As shown in figure 2, $S_{\lambda_{si}}$ and S_{T_i} are passed through a saturation function in order to maintain the control parameters in the acceptable band.

B. PI controllers

As mentioned before, the PI controllers are responsible for dynamic response of the whole controller and they are defined as:

Torque PI controller: $k_{P_{T_i}} + \frac{k_{I_{T_i}}}{s}$

Flux PI controller: $k_{P_{\lambda_{si}}} + \frac{k_{I_{\lambda_{si}}}}{s}$

The PI gains are selected such that balance among SMC and PI controllers and desired whole dynamic properties are achieved. Considering, SMC and PI controllers in addition to the decoupling term for the torque controller the reference values for direct and quadrature axis reference voltages are:

$$V_{S_i d}^* = \left(k_{P_{\lambda_{si}}} + \frac{k_{I_{\lambda_{si}}}}{s} \right) \left(e_{\lambda_{S_i}} + sat(S_{\lambda_{S_i}}) \right) \quad (23)$$

$$V_{S_i q}^* = \left(k_{P_{T_i}} + \frac{k_{I_{T_i}}}{s} \right) \left(e_{T_i} + sat(S_{T_i}) \right) \quad (24)$$

IV. TORQUE AND STATOR FLUX LEVEL SELECTION

A DTC controller based on PI-SMC is proposed for DSWIM in the previous section. Utilizing this controller, the torque and stator fluxes will follow their reference values. The reference values for stator fluxes are selected such that maximum torque per Ampere (MTPA) is attained. The torque reference value is specified such that the speed follows its reference command. The process of torque and stator flux reference values selection is as follows.

A. Flux Selection

The total air gap flux density in a DSWIM is the result of the interaction of the fluxes produced in its winding sets. The total air gap flux density in a 2/6 pole winding DSWIM is [8]:

$$\begin{aligned} B_{total} &= B_{\max_{ABC}} \sin\left(\theta_{mech} + \theta_{ABC}\right) \\ &+ B_{\max_{RST}} \sin\left(3(\theta_{mech} - \theta_d) + \theta_{RST}\right) \end{aligned} \quad (25)$$

Where $B_{max_{ABC}}$ and $B_{max_{RST}}$ are the maximum values of the flux density produced by two pole winding (ABC) and six pole winding (RST), respectively. θ_{mech} is the position measured from ABC winding set. θ_{ABC} and θ_{RST} are the position of ABC and RST windings from their references respectively and θ_d is the mechanical deviation of RST winding from ABC winding set.

For independent operation of winding sets, saturation must be avoided. The maximum total flux density must be chosen such that saturation avoided. Utilizing (25) the contours of the maximum total flux density as a function of per winding maximum flux density are obtained (Fig. 3). As illustrated in Fig. 3 for each total flux density there are a variety of per winding flux density combinations available. The flux density combination is determined to achieve MTPA.

Per winding linkage flux magnitude equals [8]:

$$\left|\lambda_{m_i}\right| = \frac{2}{P_i} N_{S_i} \left|B_i\right| lr \quad (26)$$

Where N_{s_i}, l and r are the stator winding turn number of each winding set, the stator length. If the flux leakage in the stator winding is negligible in comparison to linkage flux, (26) can be rewritten as:

$$\left|\lambda_{S_i}\right| \approx \frac{2}{P_i} N_{S_i} \left|B_i\right| lr = k_i \left|B_i\right| \quad (27)$$

Where $k_i = \frac{2}{P} N_{S_i} lr$.

The steady-state d-axis current needed to produce λ_{m_i} approximately equals [8]:

$$i_{s_i d} = \frac{\lambda_{m_i}}{L_{m_i}} \quad (28)$$

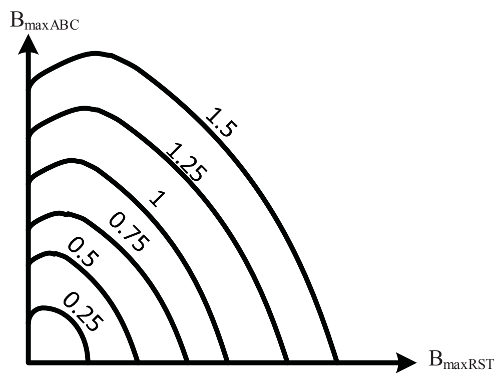

Figure 3. contours of maximum air-gap flux density

For a certain maximum stator current (I_{max_i}), the maximum quadrature axis stator current is:

$$i_{s_iq\max} = \sqrt{I^2_{\max_i} - i^2_{s_id}} \tag{29}$$

Accordingly, considering (13) and (29), the maximum achievable torque for I_{max_i}equals:

$$T_{e_i\max} = \frac{3}{2} P_i \lambda_{S_i} \sqrt{I^2_{\max_i} - i^2_{s_id}} \tag{30}$$

Form (27), (28) and (30) the maximum electromagnetic torque produced by each winding set is:

$$T_{e_i\max} = \frac{3}{2} P k_i \left|B_i\right| \sqrt{I^2_{\max_i} - \left(\frac{k_i}{L_{m_i}}\left|B_i\right|\right)^2} \tag{31}$$

The total electromagnetic torque produced by DSWIM is:

$$T_{e_{\max}} = T_{e_{ABC}\max} + T_{e_{RST}\max} = \tag{32}$$

$$\frac{3}{2} P k_{ABC} \left|B_{ABC}\right| \sqrt{I^2_{\max_{ABC}} - \left(\frac{k_{ABC}}{L_{m_{ABC}}}\left|B_{ABC}\right|\right)^2} +$$

$$\frac{3}{2} P k_{RST} \left|B_{RST}\right| \sqrt{I^2_{\max_{RST}} - \left(\frac{k_{RST}}{L_{m_{RST}}}\left|B_{RST}\right|\right)^2}$$

Now the maximum torque contours in the $B_{ABC} - B_{RST}$ plane could be plotted.

In order to perform MTPA strategy and avoid flux saturation the contour of the maximum permitted flux density should be plotted in $B_{ABC} - B_{RST}$ plane, first. Then the contours of maximum achievable torque are also plotted in the same plane. Now, the point of the interaction of the contours of maximum torque and the contour of the maximum permitted flux density, determines the reference flux density for each winding set. Finally, using (27) the reference fluxes which result in MTPA for each winding set are determined.

The parameters of the DSWIM used for simulation are given in table 1. Considering table 1 and $B_{total_{max}} = 1.25T$, the contours of the maximum available torque and maximum permitted flux are plotted in a common plane, as shown in Fig. 4. As demonstrated, the maximum achievable torque is 17 N-m. According to machine design parameter and figure 4 the reference stator flux values are:

$$\lambda^*_{S_{ABC}} = 0.65T$$

$$\lambda^*_{S_{RST}} = 0.9T$$

B. Torque Selection

The torque selection algorithm is shown in Fig. 5. As illustrated, the torque reference values for each winding set is determined such that rotor speed follows it reference signal. In this algorithm if the speed command signal is more than 5rpm or less than -5rpm, the rotor speed is compared with its reference signal and the resultant signal passes through the speed controller, which is a PI type controller, and the total torque reference value for DSWIM is produced. Now, the torque sharing between the two winding sets is performed such that overload in stator windings avoided. Since, the in the DSWIM selected for simulation, the power ratio of winding sets is unity, two windings must be equally loaded. Consequently, kABC and kRST are selected equal to 0.5. If the speed command is less than 5rpm and more than -5rpm the reference value for RST winding set equals -0.1Tload and works in generating mode and ABC winding set must provide this torque in addition to the load torque. Therefore, ABC winding set works in motoring mode and its reference value equals 1.1Tload.

Adapting this algorithm, the DSWIM can work in a wide speed range, including nominal speed, reverse nominal speed and zero speeds. This capability, is inaccessible in three phase induction machines, especially which are controlled by DTC.

V. Simulation Results

The proposed control system is simulated using MATLAB/SIMULINK. The DSWIM parameters are tabulated

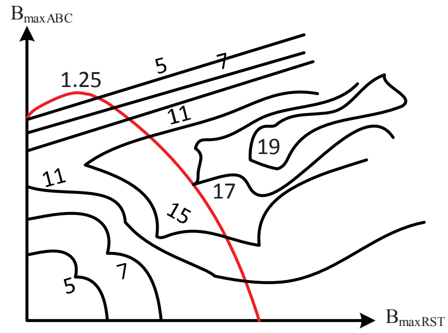

Figure 4. contours of maximum torque

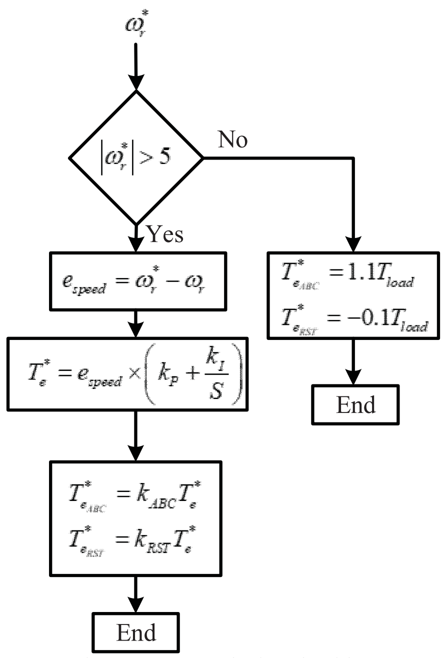

Figure 5. Torque sharing algorithm

in table 1 and the designed control parameters which are PI controller gains and SMC control parameters are given in table 2. The reference values for electromagnetic torques are determined using the algorithm discussed in the previous section. The rotor speed and the reference speed are shown in Fig. 6(a). As illustrated, in the first period the speed reference is zero and in the second and third period is nominal positive and nominal negative respectively. The error speed is demonstrated in Fig. 6(b). As shown, the rotor speed follows its reference signal properly and the speed controller has a suitable dynamic response. Figure 6 validates that DSWIM controlled by PI-SVM can work appropriately in a variety of speeds including zero speed.

The produced torque references for ABC and RST winding sets are represented in Fig. 7(a) and 7(b), respectively. As illustrated, when the reference speed is zero, the torque reference for RST winding set is negative and ABC compensates this negative torque in addition to the load torque, which is 17 N-m. When the reference speed is high, in positive and negative regions, the load torque is divided equally in two winding sets and the reference torque for both winding sets is about 8.5 N-m.

Figure The estimated and reference torque of ABC and RST winding sets are demonstrated in Fig. 8(a) and 8(b), respectively. As clarified, the produced torques follow their reference signals pleasantly and as it is expected, the DTC controller has very fast dynamic response. In addition, thanks to utilization of SMC it has respectable steady state response.

As discussed in section IV the references for stator fluxes are selected to obtain MTPA. Considering the machine design parameters and figure 4, the reference values of fluxes for ABC and RST winding sets are 0.65T and 0.9T, respectively. The operation of flux controllers is validated in Fig. 9. The estimated and reference fluxes for ABC and RST winding sets are illustrated in Fig. 9(a) and 9(b) respectively.

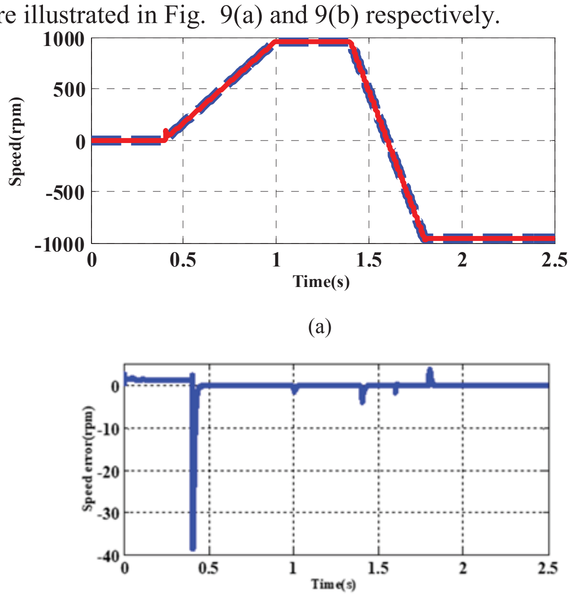

(a)

(b)

Figure 6. a)reference speed and rotor speed b) speed error

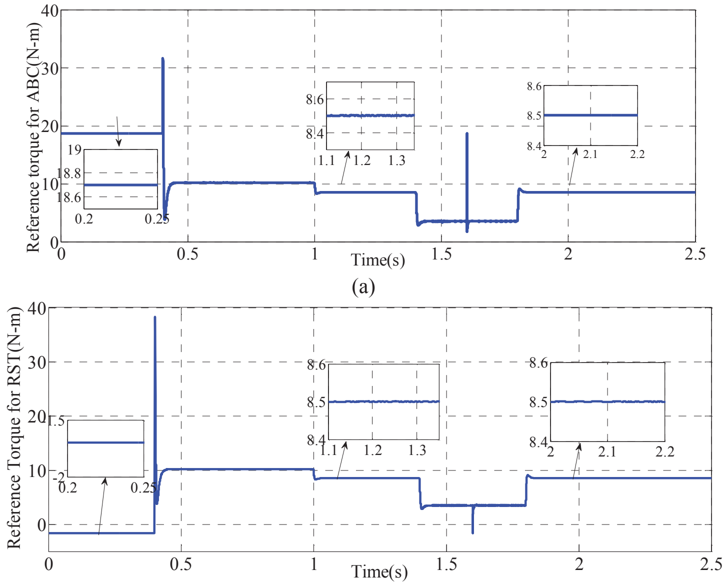

(a)

(b)

Figure 7. a) reference torque for ABC b)reference torque for RST

VI. CONCLUSION

The model of a DSWIM in synchronous reference frame presented. It is indicated that at the absence of flux saturation and at the condition that the supply frequency winding sets has a ratio equal to the pole number ratio, DSWIM can be modeled as two independent three phase induction machines. A DTC control based on PI-SMC was proposed for DSWIM. Application of both linear and variable structure controllers in the proposed control system showed a very fast and satisfactory dynamic and steady state responses for both torque and flux controllers.

A flux selection and torque sharing algorithm were proposed to achieve MTPA in a wide speed range. The simulation results verify the validity of the proposed control approach.

TABLE I. DSWIM PARAMETERS AND CONTROL PARAMETERS

DSWIM parameters	value	Controller parameters	
P_{ABC}	2	C_{1F}	0.00012
R_{SABC}	3.4Ω	C_{1T}	0.0012
R_{rABC}	0.61Ω	C_{2F}	0.00015
L_{mABC}	0.336H	C_{2T}	0.0015
L_{sABC}	0.342H	$K_{P\lambda ABC}$	50
L_{rABC}	0.342H	$K_{I\lambda ABC}$	1000
ω_{sABC}	100Π/3	$K_{P\lambda RST}$	150
P_{RST}	6	$K_{I\lambda RST}$	1000
R_{sRST}	1.9Ω	K_{PTABC}	8
R_{rRST}	0.61Ω	$K_{I\lambda ABC}$	8000
L_{mRST}	0.93H	$K_{P\lambda RST}$	10
L_{sRST}	1.02H	$K_{I\lambda RST}$	8000
L_{rRST}	1.02H		
ω_{sABC}	100Π		

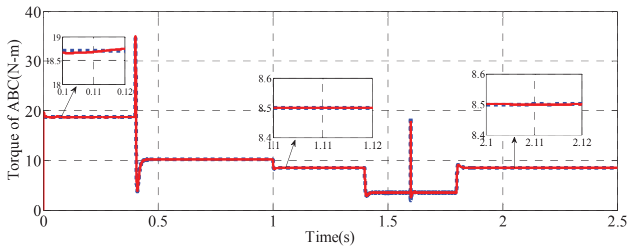

(a)

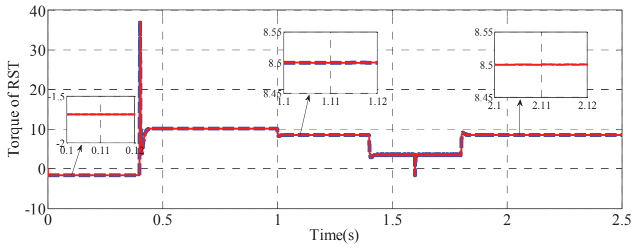

(b)

Figure 8. a)produced torque of ABC b)produced torque of RST

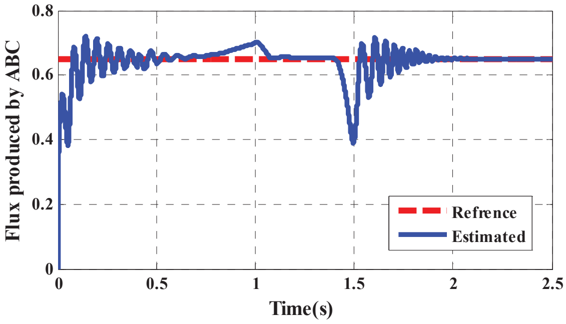

(a)

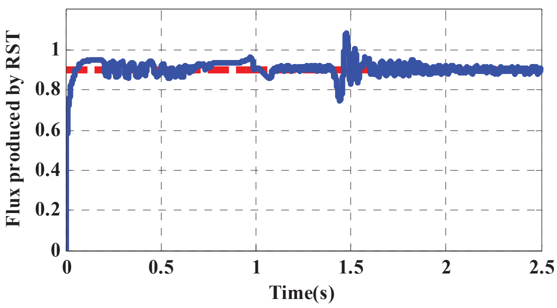

(b)

Figure 9. a) produced flux of ABC b) produced flux of RST

REFERENCES

[1] A. R. Munoz and T. A. Lipo, "Dual stator winding induction machine drive," IEEE Trans. Ind. Appl., vol. 36, no. 5, pp. 1369–1379, Sep./Oct.2000.

[2] A. Munoz-Garcia; T. A. Lipo," Dual stator winding induction machine drive," IEEE Industry Applications Conf. 1998, pp. 601-608.

[3] J. M. Guerrero and O. Ojo, "Total airgap flux minimization in dual stator winding induction machines," IEEE Trans. Power Electron., vol. 24,no. 3, pp. 787–795, Mar. 2009.

[4] Z. Wu; O. Ojo; J. Sastry, "Control of a dual stator winding induction machine as a source of dc power," IEEE Industry Applications Conf, 2005, pp. 1089-1096.

[5] Z. Wu, O. Ojo and J. Sastry, "High-performance control of a dual stator winding DC power induction generator," IEEE Trans. Ind. Appl.,vol. 43, no. 2, pp. 582–592, Mar./Apr. 2007.

[6] O. Ojo and Z. Wu, "Speed control of a dual stator winding induction machine," in Proc. IEEE APEC, Feb./Mar. 2007, pp. 229–235.

[7] O. Ojo, Z.Wu, and G. Dong, "MRAS speed estimation and full-order flux observer for dual stator winding induction motor drives," in Proc. IEEE Power Electron. Spec. Conf., 2007, pp. 2428–2435.

[8] J. M. Guerrero; O. Ojo," Flux level selection in vector-controlled dual stator winding induction machines," IET Electric Power Applications, vol. 3, no. 6, pp. 562–572, 2009.

[9] M. Guerrero and O. Ojo, "Performance optimization in dual stator winding induction machines through flux partitioning," in Proc. IET Power Electron., Mach. Drives Conf., 2008, pp. 696–700.

[10] J. M. Guerrero and O. Ojo, "Total airgap flux minimization in dual stator winding induction machines," IEEE Applied Power Electronics Conf. 2008, pp. 1132-1138.

[11] J. M. Guerrero and O. Ojo, "Air-gap flux density optimization in dual stator winding induction machines," in Proc. IEEE Power Electron. Spec. Conf., 2008, pp. 3767–3773.

[12] I. Takahashi and T. Noguchi, "A new quick response and high efficiency control strategy of an induction motor," in Conf. Rec. IEEE-IAS Annu. Meeting, 1985, pp. 495–502.

[13] C. Lascu, I. Boldea, and F. Blaabjerg, "A modified direct torque control for induction motor sensorless drive," *IEEE Trans. Ind. Applicat.*, vol.36, pp. 122–130, Jan./Feb. 2000.

[14] C. Lascu, I. Boldea, and Frede Blaabjerg, "Variable-Structure Direct Torque Control—A Class of Fast and Robust Controllers for Induction Machine Drives," *IEEE Trans. Ind. Electronics.*, vol.51, pp. 785–792, August.2004.

[15] S. M. Fazeli, H. W. Ping, M. A. Rahman, J. Soltani, H. A. Zarchi, , "A Modified DTC of speed sensorless IPMSM drives using variable structure approach," in Conf. Industrial Electronics and Applications (ICIEA), 2010, pp. 701-706.